Self-study: Stochastically forced oscillators with sigmoid-type saturation

It is also interesting to consider the case of a sigmoid-type flame response nonlinearity, which is much closer than the cubic-type saturation leading to the Van der Pol oscillator model, and look at the corresponding acoustic pressure statistics. This is for example the case of the function arctangent as depicted in figure 3. The Simulink model of the self-sustained oscillator given by Eq. (20) is now set with

$$f(\eta_j, \dot{\eta}_j) = \dot{\eta}_j \left(\beta - \alpha - \frac{\kappa \eta_j^2}{1 + (\kappa/\beta)\, \eta_j^2} \right), \tag{38}$$

which corresponds to $q_c = \beta \sqrt{\beta/\kappa}\, \mathrm{atan}(\sqrt{\kappa/\beta}\, \eta_j)$. These expressions can be compared to the Van der Pol formulation leading to Eq. (22). Using the same parameters for α, β and κ as the ones taken for the simulations of the Van der Pol model, simulations of the oscillator with arctangent-type saturation can be performed. The corresponding results are shown in figure 8. Note that simulated time traces are displayed on a wider scale compared to the Van der Pol case presented in figure 4.
The PDF are computed from the histograms of the 240 seconds simulated time traces. One can see that the PDF are qualitatively the same as the ones obtained from the Van der Pol model. In fact, one can also derive the amplitude equation for this type of nonlinearity. This is done by following the deterministic and stochastic averaging procedure that has been presented for the Van der Pol oscillator. It gives

$$\dot{A} = -\frac{\partial \mathcal{V}}{\partial A} + \zeta, \tag{39}$$

with $-\partial \mathcal{V}/\partial A = \mathcal{F}(A)$ and

$$\mathcal{F}(A) = -\frac{\alpha}{2} A + \frac{\Gamma}{4\omega_j^2 A} + \beta A \left(\frac{\sqrt{1 + \kappa A^2/\beta} - 1}{\kappa A^2/\beta} \right). \tag{40}$$

The corresponding stable deterministic limit cycle amplitude (for $\Gamma = 0$) is given by $\sqrt{8\nu/\kappa}\,(1 + 2\nu/\alpha)$. From these expression, one can express the potential

$$\begin{aligned} \mathcal{V}(A) = & \frac{\alpha}{4} A^2 - \frac{\Gamma}{4\omega_j^2} \ln A - \frac{\beta^2}{\kappa} \sqrt{1 + \kappa A^2/\beta} \\ & + \frac{\beta^2}{\kappa} \ln \left(1 + \sqrt{1 + \kappa A^2/\beta} \right) \end{aligned} \tag{41}$$

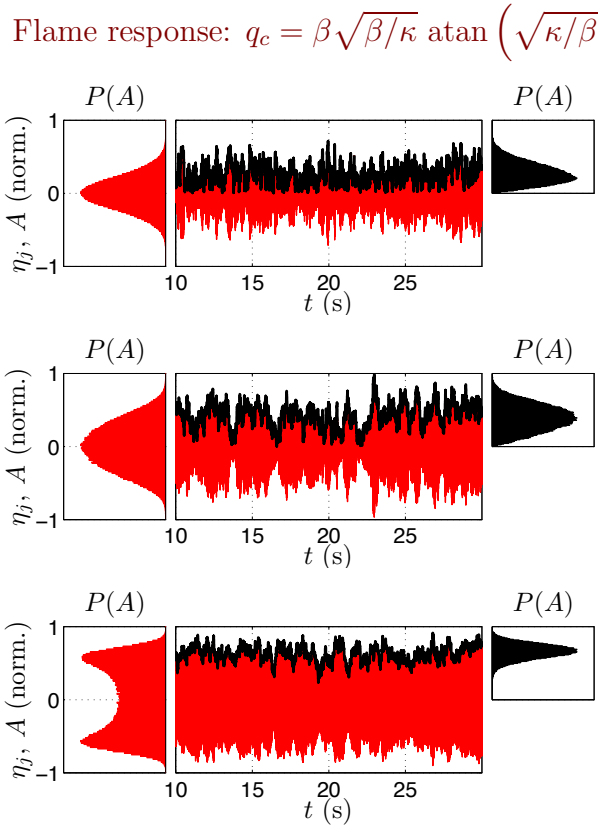

Figure 8: Time domain simulations (60 seconds) of the oscillator with arctangent nonlinearity given by Eqs. (20) and (38), for different linear growth rates ν. The signals are normalized by the maximum amplitude reached during the simulation. Note also that results are displayed over a longer time scale for the arctangent saturation case than for the Van der Pol case presented at Fig. 4. For these simulations, $\beta = 60$ rad/s, $\kappa = 3.4$, $\Gamma = 10^7$ and $\omega_j = 2\pi f_j$ with $f_j = 120$ Hz. Three values of the damping α are considered (72, 60 and 48 rad/s). These simulations respectively correspond to a linearly stable thermoacoustic system (top row), a marginally stable one when damping α balances the linear driving from the flames β (middle row), and a stochastic limit cycle when the growth rate $\nu = (\beta - \alpha)/2$ is positive (bottom row). On each rows, from left to right: the PDF of the simulated acoustic signal $P(\eta)$, a portion of the time series and its envelope (black curves) and the PDF of this envelope $P(A)$.

and therefore obtain an analytical expression for the PDF of this stochastic Hopf bifurcation using Eq. (14). These theoretical results are summarised in figure 9, and it is interesting to compared them with the Van der Pol model given in figure 5, which is the exact 3$^{\mathrm{rd}}$ order approximation of this arctangent saturation model.

As an exercise, you can make use of the matlab script and corresponding Simulink model for the Van der Pol oscillator and adapt them to generate Figure 9. The simulated signal can be plotted using Matlab or the oscilloscope in Simulink to visualize the transient at the beginning of the simulation.

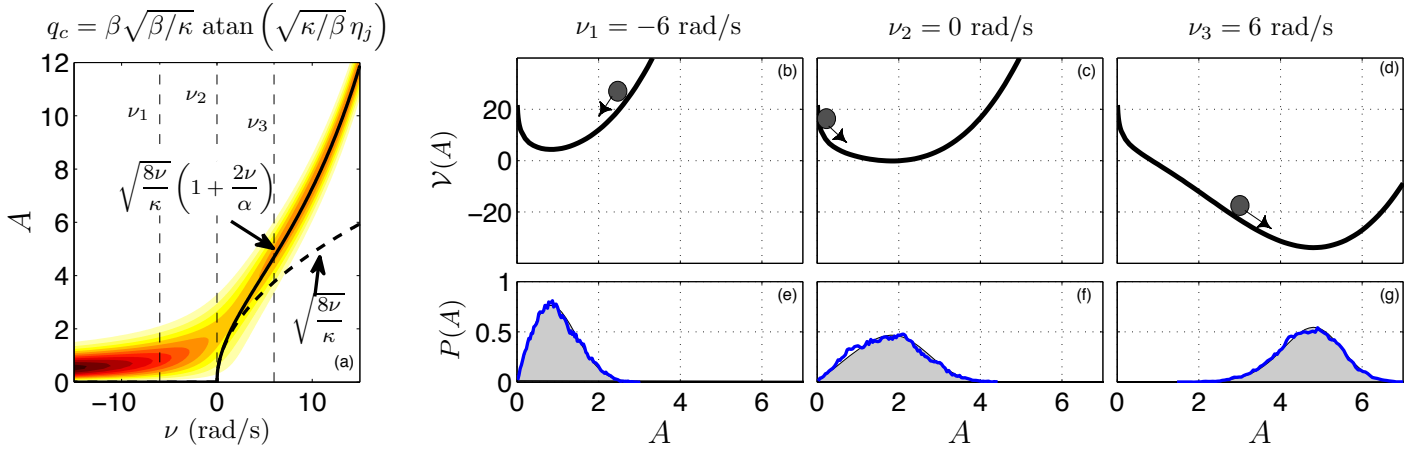

Figure 9: (a) Stochastic bifurcation diagrams associated with the acoustic amplitude dynamics for nonlinear damping resulting from arctangent-type feedback. The bifurcation parameter is the growth rate ν that has been varied by setting different values of the linear damping α, while the other parameters ω, κ and Γ are fixed. A contour plot of the theoretical probability density function given by Eq. (14) is shown together with the deterministic bifurcation curve (solid line). (e-g) $P(A)$ at selected linear growth rates ν_i with a variation from linearly stable ($\nu < 0$) to linearly unstable ($\nu > 0$) conditions. The shaded areas are the theoretical PDF and the thick blue lines correspond to the PDF from the normalised histograms of the simulated stochastic oscillators (see Fig. 8). (b-d) corresponding potential and related contributions.